GASTROINTESTINAL

Feasibility and reproducibility of T2 mapping and DWI for identifying malignant lymph nodes in rectal cancer

Yu-xi Ge [1] · Shu-dong Hu [1] · Zi Wang [1] · Rong-ping Guan [1] · Xin-yi Zhou [2] · Qi-zhong Gao [3] · Gen Yan [4]

Abstract

Objectives To evaluate the diagnostic value and reproducibility of T2 mapping versus apparent diffusion coefficients (ADC) for identifying malignant lymph nodes in patients with non-mucinous rectal adenocarcinoma.

Methods High-resolution magnetic resonance imaging, diffusion-weighted imaging, and T2 mapping were performed on patients with suspected metastatic lymph nodes in the mesorectum or around the superior rectal artery with a short-axis diameter of 4–10 mm. The T2 and ADC values of pathology-confirmed metastatic versus non-metastatic lymph nodes were compared using the independent-samples t test and receiver operating characteristic curves. Intra- and inter-observer reproducibility were tested. The cutoff value for T2 relaxation time was determined.

Results In total, 67 lymph nodes underwent histological analysis, with 24 in the non-metastatic and 43 in the metastatic groups. Intra- and inter-observer agreements for T2 values were 0.999 and 0.998, respectively, which were higher than the ADC values of 0.924 and 0.844, respectively. The mean T2 and ADC values for metastatic lymph nodes (65 ± 7.8 ms and $1.17 \pm 0.16 \times 10^{-3}$ mm^2/s, respectively) were significantly lower than for benign lymph nodes(83 ± 5.7 ms and $1.29 \pm 0.15 \times 10^{-3}$ mm^2/s, respectively). T2 values had a higher AUC value of 0.990 than the AUC value for ADC of 0.729. With a cutoff value of 77 ms, sensitivity and specificity for T2 values were 95% and 96%, respectively.

Conclusions T2 mapping had higher diagnostic efficacy and reproducibility than ADC and may be useful in differentiating metastatic from non-metastatic lymph nodes in rectal cancer.

Key Points

• *Mean T2 values were significantly shorter for malignant versus benign LNs in patients with non-mucinous rectal adenocarcinoma.*
• *The diagnostic efficacy and reproducibility of T2 values were excellent and superior to ADC values.*

Keywords Magnetic resonance imaging · Rectal cancer · Lymph nodes · Metastatic

Abbreviations

ADC	Apparent diffusion coefficient
AUC	Area under the curve
CRT	Chemoradiotherapy
DWI	Diffusion-weighted imaging
FOV	Field of view
ICC	Intraclass coefficient
LN	Lymph node
LNM	Lymph node metastasis
LoA	Limits of agreement
MRI	Magnetic resonance imaging
ROC	Receiving operating characteristic
ROI	Region of interest
T2WI	T2-weighted imaging
TE	Echo time
TME	Total mesorectal excision

✉ Qi-zhong Gao
gaoqizhong@sina.com

✉ Gen Yan
gyan@stu.edu.cn

1 Department of Radiology, Affiliated Hospital of Jiangnan University, 200 Huihe Road, Wuxi, Jiangsu, China

2 Department of Pathology, Affiliated Hospital of Jiangnan University, 200 Huihe Road, Wuxi, Jiangsu, China

3 Department of Gastrointestinal Surgery, Affiliated Hospital of Jiangnan University, 200 Huihe Road, Wuxi 214000, Jiangsu, China

4 Department of Radiology, The Second Affiliated Hospital of Xiamen Medical College, 556 Shengguang Road, Xiamen 361021, Fujian, China

Introduction

Since neoadjuvant chemoradiotherapy (CRT) followed by radical total mesorectal excision (TME) has become the standard of care for patients with locally advanced rectal cancer [1], accurate identification of lymph node (LN) involvement has become crucial for prognostic and therapeutic decision-making [2]. Unfortunately, preoperative characterization of metastatic lymph node involvement remains extremely challenging for radiologists. Currently, high-resolution magnetic resonance imaging (MRI) is most commonly used for assessments of lymph node status. While the size and morphology of lymph nodes determined on conventional MR images are often used to evaluate the extent of malignant disease, this imaging modality does not have a satisfactory sensitivity nor specificity for these evaluations because malignant disease may be present even in very small nodes. In addition, identifying tumor-related morphological features, including capsular invasion, central necrosis, and chemical shift effects, is often dependent on the subjective judgments of different radiologists [3–5].

MRI is considered to be an accurate test to define locoregional clinical staging of rectal cancer [6]. Diffusion-weighted imaging (DWI), an important functional imaging modality widely used in preoperative staging of rectal cancer, can be helpful for differentiation of LN status [7]. Although most studies have reported significantly higher apparent diffusion coefficients (ADC) for benign nodes than for malignant nodes [8–10], malignant and benign nodes have also been reported to have significant overlap in ADC values [11]. Therefore, a more objective and accurate quantitative method needs to be identified for distinguishing benign from malignant lymph nodes.

Among all MRI sequences, T2-weighted images are considered to be the most effective at demonstrating the detailed microstructure and internal morphology of normal lymph nodes [12], often enabling identification of small nodes measuring only 2–5 mm [5]. Schnall et al [13] have suggested that a low nodal signal intensity on T2-weighted images may be a predictor of tumor involvement. Other studies [5, 14] have reported that nodes with mixed signal intensities are likely to contain areas of necrosis or extracellular mucin corresponding to metastatic adenocarcinomas. While studies have indicated that low or heterogeneous signals may be associated with tumor involvement, identification of these findings can be subjective and can vary greatly depending on the tissue type. T2-weighted images demonstrate the relative, but not the absolute, T2 signal intensity of the tissue. If quantitative T2 values of lymph nodes can be accurately measured, these values may be helpful for distinguishing benign from malignant lymph nodes.

T2 mapping is a quantitative MRI technique used to measure altered water binding related to physiological or pathological macromolecular environmental changes. T2 mapping is performed by acquiring images of the same slice at multiple echoes with pixel-by-pixel fitting of a T2 relaxation curve [15]. Quantitative T2 relaxation times have been widely used in evaluations of diseases of the cartilage and musculature [16], myocardium [17], and nervous system [18]. T2 mapping has also been used for differentiating pleomorphic adenomas from Warthin's tumors [19] and for distinguishing benign from malignant breast lesions [20]. It has also been reported that quantitative T2 values are suitable for distinguishing prostate cancer from normal gland tissue or benign prostatic hyperplasia nodes [21].

Although previous studies have proven the utility and feasibility of T2 mapping for evaluations of several tumor types, few studies have investigated the utility of T2 mapping in lymph node examinations. The aim of this study was to determine quantitative T2 values that could differentiate benign from malignant lymph nodes in patients with non-mucinous rectal adenocarcinoma, to compare them to corresponding ADC values, and to evaluate their diagnostic efficacy and reproducibility for the characterization of benign and malignant lymph nodes.

Materials and methods

Patients

Our prospective study was approved by the Medical Ethics Committee of our institution and conformed to the tenets of the Declaration of Helsinki. Written informed consent was obtained from all patients. Between November 2017 and December 2019, 134 patients with biopsy-proven rectal adenocarcinoma were identified. All patients underwent MRI examination with conventional sequences and DWI. Forty-one patients who met the enrollment criteria but did not have sufficient lymph nodes in the mesentery fascia or around the superior rectal artery were excluded. T2 mapping scans of selected lymph nodes were then performed on the remaining 93 patients. Among these patients, two were excluded because of poor MRI quality, nine were excluded because they did not undergo a scheduled curative surgery in our gastroenterology department, four were excluded because they had a diagnosis of mucinous adenocarcinoma, and 31 were excluded because they were receiving neoadjuvant chemoradiotherapy. Thus, our prospective study enrolled a total of 46 patients, including 25 males and 21 females with a mean age of 60.2 years (range 27–81 years) and 67 examined lymph nodes. The average time between MRI examination and surgery was 5 days (range 1–10 days).

Imaging technique

A 3.0 Tesla MR system (750w; GE) with a 16-channel phased-array body coil was used for image acquisition. All

patients were scanned in the supine position with a feet-first orientation. Patient rectal preparation involved fasting and taking oral polyethylene glycol electrolyte solution 6–8 h before the examination. Unless contraindicated, 20 mg of raceanisodamine hydrochloride (Minsheng Pharmaceutical Group Co.) was slowly injected intramuscularly into the buttocks to prevent bowel peristalsis approximately 10–15 min before the examination.

Axial, sagittal, and coronal high-resolution T2-weighted and DWI images were obtained. When the tumor was located, the location line was determined to be parallel to the tumor, and the field of view (FOV) was expanded to include the tumor and regional lymph nodes. For DWI, the oblique axial planes were oriented orthogonal to the tumor base on high-resolution T2-weighted images. FOV settings were determined to include tumors and all mesenteric and fascial lymph nodes. For coronal T2 mapping, the lymph nodes to be evaluated were determined by a senior radiologist using the criteria for selection of lymph nodes (see below). The parameters for all MRI protocols are shown in Table 1.

Image measurements

Acquired images were transferred to a workstation (ADW 4.6 workplace; General Electric) where the ADC and T2 values were calculated. A junior radiologist and a senior radiologist (Z.W. and S.H., with 5 and 18 years of work experience, respectively), who specialize in gastrointestinal tumors and were blinded to the study design and diagnoses, performed the measurements. The senior radiologist repeated the measurement 2 weeks later. For ADC determination, the region of interest (ROI) was drawn freehand on DWI along the border of the lymph node on the slice in which the lymph node showed the greatest diameter in reference to the corresponding T2-weighted image. For T2 values, the freehand ROI was drawn along the border of the lymph node on the slice with the greatest diameter in which the echo time (TE) was 64.6 ms in order to

provide a clearer contrast in reference to the corresponding coronal T2-weighted image. Correspondingly, the T2 values of the ROI were calculated on the color-coded T2 mapping.

Lymph node localization

When the high-resolution T2WIs were scanned, appropriate lymph nodes were carefully identified on axial images by a senior radiologist. The criteria for selection of lymph nodes were as follows: (1) a short diameter of 4–10 mm, (2) location in the mesentery fascia or around the superior rectal artery, and (3) if there were multiple lymph nodes that met the preceding two conditions, the lymph node closest to the rectal tumor was selected. If the selected lymph node was located in the mesenteric fascia, the following information was provided by the radiologist: number, location, orientation on a clock face, and short diameter. If the selected lymph node was located around the superior rectal artery, the radiologist provided information about the side of the superior rectal artery (including the left and right branches) in which the lymph node was located, as well as its diameter. The short diameters of lymph nodes were measured on axial T2-weighted images at the workstation. Coronal T2 mapping position was identified according to sagittal and axial images on T2WI on the MRI scanner operation interface to ensure that the selected lymph nodes and tumor were included in the scanning field. Before TME, a surgeon with expertise in colorectal cancer confirmed the selected nodal positions on the MR images and the recorded information with the senior radiologist. After the TME operation, the selected lymph nodes were carefully identified and resected by the surgeon. The lymph nodes were then fixed in a formalin solution for 48 h and routinely stained with hematoxylin-eosin. They were then categorized into either the metastatic or the non-metastatic group by a pathologist who was blinded to the MRI results.

Table 1 MR sequence parameters

Parameters	T2WI			DWI	T2 mapping
Orientation	Sagittal	Axial	Coronal	Axial	Coronal
Sequence	Spin echo	Spin echo	Spin echo	EPI	Multiecho spin echo
TR (ms)	6222	5367	5367	3648	1500
TE (ms)	107	107	107	70	8.1–64.6 ($\triangle$ = 8.1 ms)
FOV (mm)	260	180	180	360	320–340
Slice thickness (mm)	4.0	3.0	3.0	5.0	3.0
b value (s/mm^2)	-	-	-	0, 800	-
No. of slices	20	30–37	30	21	19
Acquisition time (min:s)	3:50	3:10–3:50	2:36	1:03	4:03

DWI, diffusion-weighted imaging; *FOV*, field of view; *TE*, echo time; *TR*, repetition time; *T2WI*, T2-weighted images; *EPI*, echo planar images

Statistical analyses

Statistical analyses were performed using Statistical Package for the Social Sciences (SPSS, version 22.0, IBM) and MedCalc Statistical Software (version 18.2). Intra- and inter-observer agreements for T2 and ADC values were analyzed by estimating the intraclass correlation coefficients (ICCs). The ICC values were interpreted as follows: poor inter-rater agreement < 0.40; fair = 0.40–0.59; good = 0.60–0.74; and excellent = 0.75–1.00. Bland-Altman plots were also constructed, and the limits of agreement (LoAs) were estimated from the plots. According to the results of the one-sample Shapiro-Wilk test, continuous data were expressed as either means ± standard deviations (SDs) or medians with interquartile ranges (IQRs). The independent-samples t test and the Mann-Whitney U test were used for comparisons of normally and non-normally distributed data, respectively. Receiver operating characteristic (ROC) curves were constructed for T2 and ADC values, and the DeLong test was used to compare the differences between the two curves. Cutoff values were determined, and the associated sensitivities and specificities were calculated.

Results

Histopathologic findings

Sixty-seven lymph nodes were obtained from 46 patients. Twenty-one patients had two lymph nodes resected, and 25 patients had one lymph node resected. Pathologic analysis identified 24 non-metastatic lymph nodes and 43 metastatic lymph nodes. The mean short-axis diameter of malignant LNs (6.9 ± 2.1 mm) was significantly longer than for benign LNs (5.3 ± 1.1 mm) ($p < 0.001$).

Intra- and inter-observer agreement

Intraclass correlation coefficients (ICC) for T2 and ADC values displayed excellent intra- and inter-observer agreements (Table 2). For both intra- and inter-observer agreements, T2 values had higher ICC values than ADC values. Measured values for all included LNs are summarized in Table 2. The Bland-Altman plots in Fig. 1 show that the points in each plot tended to distribute around the mean difference line, with fewer points outside of − 1.96 SD to + 1.96 SD of

the mean for T2 values than for ADC values. The first measurements obtained by the senior radiologist were used in further analyses because these T2 and ADC values had excellent inter-observer agreements.

Diagnostic efficiency and comparison

The mean T2 values of metastatic lymph nodes (65 ± 7.8 ms) were significantly lower than for benign lymph nodes (83 ± 5.7 ms) ($p < 0.001$), as shown in Table 3. The mean ADC value for metastatic lymph nodes ($1.17 \pm 0.16 \times 10^{-3}$ mm²/s) was significantly lower than for benign lymph nodes ($1.29 \pm 0.15 \times 10^{-3}$ mm²/s) ($p = 0.004$), as shown in Table 3. T2 and ADC values for metastatic and benign lymph nodes are shown in Figs. 2 and 3, respectively. The area under the curve (AUC) derived from the ROC curves of T2 values exhibited excellent diagnostic performance (0.990) for discriminating metastatic from non-metastatic LNs (Fig. 4). ADC values exhibited moderate performance (0.729) for discriminating metastatic from non-metastatic LNs. The two ROC curves showed a significance level of $p = 0.0001$. When 77 ms was used as a T2 cutoff value, the sensitivity and specificity were 95% and 96%, respectively.

Discussion

Identifying metastatic LNs in patients with rectal cancer has been a longstanding challenge for radiologists because of size and morphology overlap between benign and malignant LNs. Our study showed that T2 relaxation times of malignant LNs were significantly lower than for benign LNs. The diagnostic efficacy and reproducibility of T2 values for the identification of malignant lymph nodes were excellent and superior to that of ADCs. Based on our study, a cutoff value of 77 ms for T2 mapping is proposed to distinguish benign from malignant LNs. To the best of our knowledge, our study is the first to use T2 mapping to characterize malignant and benign LNs in patients with non-mucinous rectal adenocarcinoma.

Quantitative parameters of functional MRI provide useful information about tissue microenvironment beyond morphological features, including dynamic contrast-enhanced (DCE) imaging parameters [22], ADC values [9, 23], and intravoxel incoherent motion (IVIM) parameters [24]. These parameters have potential utility in identifying LN status, with AUCs

Table 2 Intra- and inter-observer agreement of T2 and ADC values for selected lymph nodes

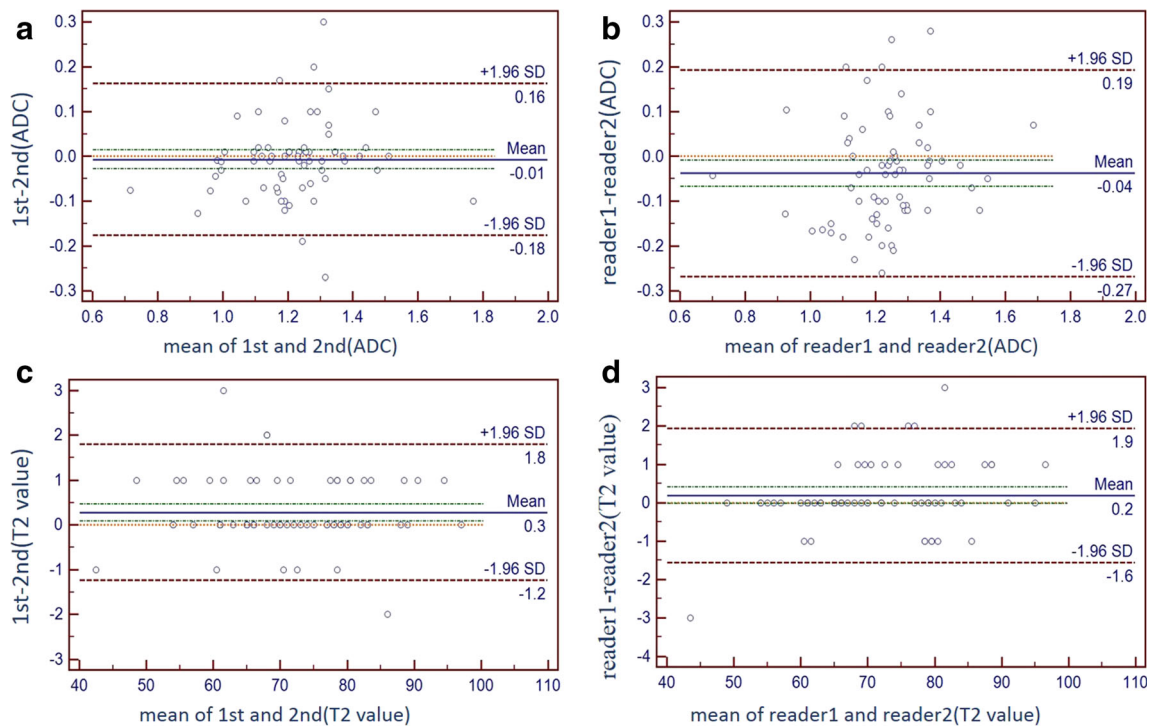|	Reader 1 (1st time)	Reader 1 (2nd time)	Reader 2	Intra-observer (95% CI)	Inter-observer (95% CI)
T2 value (ms)	72 ± 11.2	71 ± 11.2	72 ± 10.9	0.999 (0.998–0.999)	0.998 (0.997–0.999)
ADC ($\times 10^{-3}$ mm²/s)	1.21 ± 0.17	1.22 ± 0.18	1.25 ± 0.15	0.924 (0.876–0.952)	0.844 (0.747–0.904)

Fig. 1 Bland-Altman plots of apparent diffusion coefficients (ADCs) and T2 values for 67 lymph nodes with short-axis diameters between 4–10 mm. **a** Comparison of ADCs measured on both sides by the same observer and (**b**) by two different observers. **c** Comparison of T2 values measured on both sides by the same observer and (**d**) by two different observers. X-axis is the difference in parametric values. Y-axis is the mean value

ranging from 0.743–0.897. In our study, T2 mapping had an even higher AUC value of 0.990 when calculating the absolute T2 relaxation time of each lymph node.

Calculation of T2 relaxation time allows for a quantitative evaluation of investigated structures. T2 relaxation time is affected by many factors, including water content and interaction with collagen fibers [25]. There are two states of water molecules in lymph nodes, free water or bound water. T2 relaxation time prolongation is related to increases in tissue water content, especially free water molecules. Several studies have applied T2 mapping techniques to the differentiation of malignant from benign tumors in organs. In the parotid gland, malignant tumors show significantly shorter T2 relaxation times than benign growths [19], with similar results found in breast tumors [20]. Our study also demonstrated that T2 relaxation times of malignant LNs were significantly shorter than inflammatory LNs. These malignant tumors likely exhibited hypercellularity, which can reduce the extracellular space and thus decrease the tissue free water. On the other hand, quantitative T2 mapping in cases of myositis reveal higher

T2 values (16), probably due to the increased amount of free water in the muscle. Therefore, we speculate that inflammatory LNs contain more free water, while metastatic LNs contain more bound water. This difference may account for the longer T2 relaxation times that were observed in inflammatory LNs than in metastatic LNs.

T2 mapping, which has been shown to be a robust technology for measurements of myocardial T2 values using a 3.0 Tesla [26], can more clearly show the boundaries and microstructures of LNs than DWI. Radiologists can draw the ROI directly on the original T2 mapping images because of the higher resolution contrast, especially on the map in which the TE is 64.6 ms. On the other hand, the ROI for DWI must be drawn by reference to the corresponding T2WI due to a lower resolution that cannot determine the boundaries of lymph nodes. Our results show that observer consistency for DWI is not as accurate as for T2 mapping, which may largely be due to measurement errors. In addition, ADC value determination is not as effective as T2 values for the identification of LN status. These results

Table 3 Comparison of ADC and T2 values for non-metastatic and metastatic lymph nodes

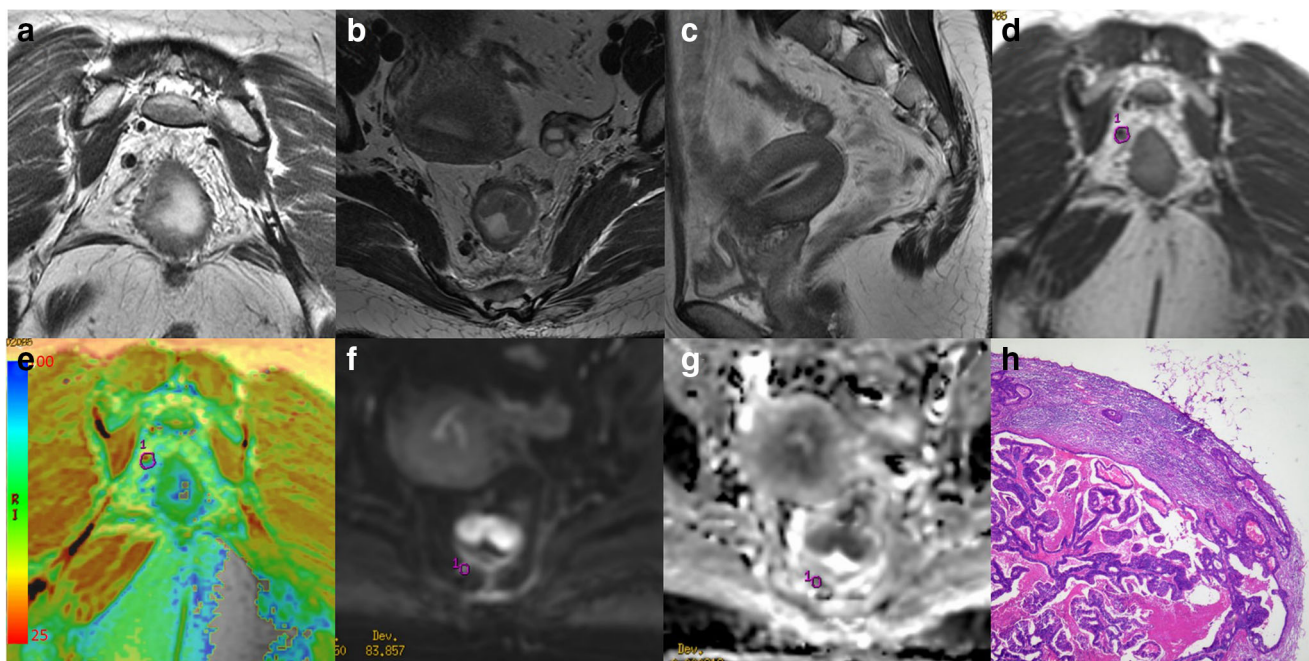|	Non-metastatic LNs (n = 24)	Metastatic LNs (n = 43)	p values
T2 values (ms)	83 ± 5.6	65 ± 7.8	0.000
ADC ($\times 10^{-3}$ mm^2/s)	1.29 ± 0.15	1.17 ± 0.16	0.004

Fig. 2 A 56-year-old female patient with a suspected metastatic lymph node from a primary rectal cancer. **a** Coronal, (**b**) axial, and (**c**) sagittal views of T2-weighted imaging showing a lymph node with a 6-mm diameter in the mesorectum at 7 o'clock. **d** The freehand ROI was drawn on the image with a TE of 64.6 ms. **e** The T2 value of 62 ms was calculated correspondingly, which appears red on the color-coded image. **f** On DWI image, the lymph node demonstrated a slightly higher signal, (**g**) and the corresponding ADC value was 1.52×10^{-3} mm^2/s. **h** Metastatic adenocarcinoma was noted in this lymph node (hematoxylin-eosin stain, original magnification × 40)

may be explained, at least in part, by the fact that diffusion limits can also be found in inflammatory LNs [11].

There are some important considerations to keep in mind when evaluating the scanning positions of T2 mapping. First,
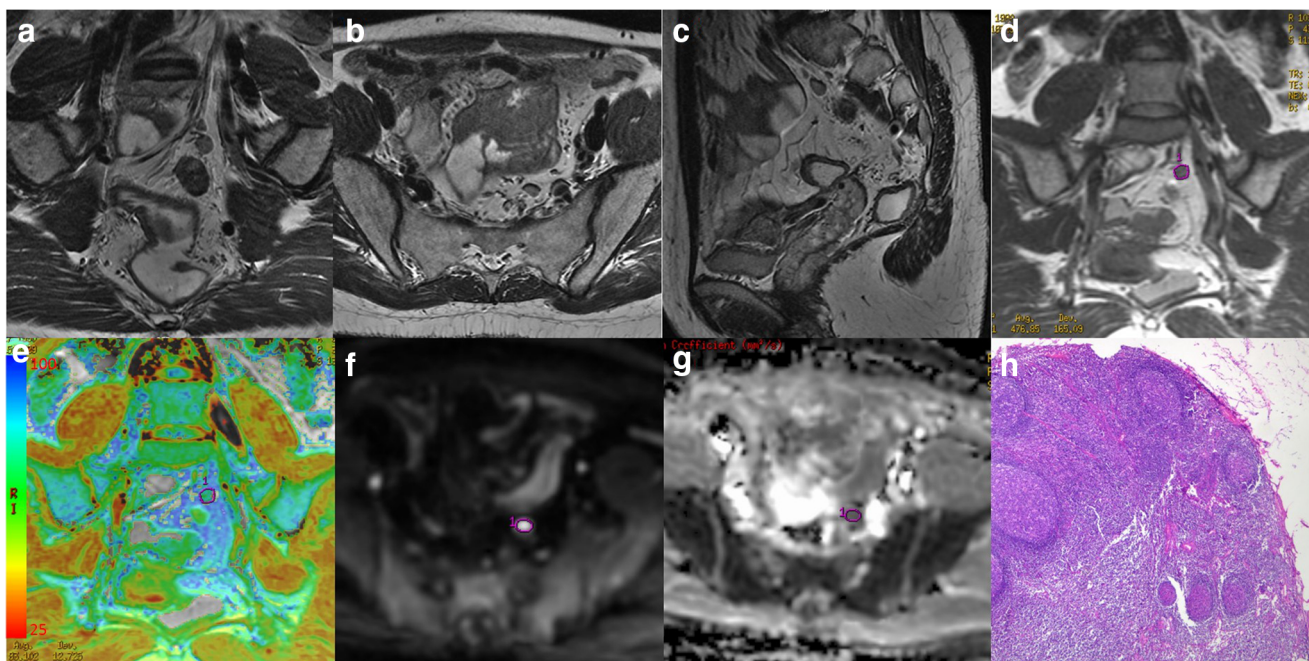

Fig. 3 A 36-year-old female patient with a suspected metastatic lymph node from a primary rectal cancer. **a** Coronal, (**b**) axial, and (**c**) sagittal views of T2-weighted imaging showing a lymph node with a 8-mm diameter around the superior rectum artery. **d** The freehand ROI was drawn on the image with a TE of 64.4 ms. **e** The T2 value of 83 ms was calculated correspondingly, which appears on the blue-coded image. **f** On the DWI image, the lymph node demonstrated an obviously high signal, and (**g**) the corresponding ADC value was 1.24×10^{-3} mm^2/s. **h** Normal lymph cells and lymphoid follicle structures were found in this lymph node (hematoxylin-eosin stain, original magnification × 40)
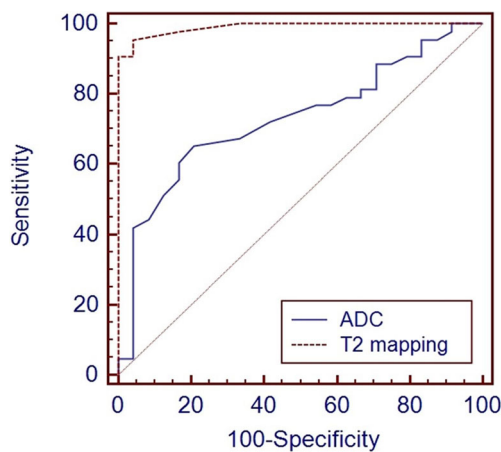
Fig. 4 Receiver operating characteristic (ROC) curves for discriminating metastatic from non-metastatic lymph nodes (LNs) for T2 (dashed line) and ADC values (solid line). The area under the ROC curve (AUC) of the T2 value was significantly higher than for the ADC value (AUC T2 value = 0.990, AUC ADC = 0.729, p = 0.0001)

the axial position may only cover one rectal region when the slices are fixed. Second, the sagittal position is not conducive to visually observe the lymph nodes located on the left or right side of the rectum. Third, the coronal position may allow more LN regions to be included in the scanning field. In addition, the coronal position appears to be most consistent with specimens that are removed after surgery and is superior for allowing surgeons to isolate selected LNs. In our study, 4–10 mm was used as the criteria for the range of short diameters for lymph nodes. This range was chosen because a former study demonstrated that a cutoff value of 10 mm for lateral pelvic lymph node metastases had a specificity reaching 98.5% [27]. In our study, 4 mm was used as the minimum cutoff value to ensure the accuracy of measurements.

Several studies have compared LN status determination using MRI findings versus pathology results [14, 22]. Most of these studies, however, were retrospective and therefore could not directly assess whether the LNs detected on MRI were the same as those assessed by histopathology. Moreover, mismatches may have occurred when multiple lymph nodes were first localized by a radiologist on MRI and then resected by a surgeon, since multiple enlarged lymph nodes are commonly found around an area of rectal cancer. Hence, we prospectively selected only one lymph node in each region for each patient, and the location information about lymph nodes was carefully recorded by a radiologist in order to facilitate accurate localization by the surgeon.

There were several limitations to this study. First, the patient cohort and number of studied LNs were relatively small. As a result, we did not compare the diagnostic efficacy of T2 mapping for different diameters of LNs. Moreover, in our study, a basic T2 mapping sequence was used and it was time consuming to evaluate an entire tumor area plus regional

lymph nodes, especially when the tumor size is large. Compared with DWI, the acquisition time of T2 mapping might be a limitation when applied to clinical practice. However, accelerated T2 mapping, a new reconstruction algorithm combined with a dedicated k-space under sampling pattern, may provide more accurate information and more time-efficient than conventional T2 mapping in the prostate [28]. Therefore, we believe that further optimization of the sequence might be even better in making a difference between malignant and benign LNs. Third, high-resolution T2 mapping was not attempted. A recent study observed that T2 maps could distinctly resolve the normal colorectal wall into eight layers corresponding with the histologic layers ex vivo [29]. Therefore, we believe that it is possible to display lymph nodes smaller than 4 mm more clearly with T2 mapping.

In conclusion, our study demonstrated that T2 relaxation times were significantly shorter in malignant versus benign LNs in patients with non-mucinous rectal adenocarcinoma. The diagnostic efficacy and reproducibility of T2 values were excellent and superior to the use of ADC values. Therefore, T2 mapping may serve as an incremental imaging biomarker for the identification of metastatic LNs.

Compliance with ethical standards

Guarantor The scientific guarantor of this publication is Gen Yan, M.D., Ph.D.

Conflict of interest The authors of this manuscript declare no relationships with any companies, whose products or services may be related to the subject matter of the article.

Statistics and biometry Shu-dong Hu was kindly provided statistical advice for this manuscript.

Informed consent Each enrolled patient was asked to sign an informed consent form.

Ethical approval Institutional Review Board approval was obtained.

Methodology
• prospective
• diagnostic study
• performed at one institution

References

1. Benson AB, Venook AP, Al-Hawary MM et al (2018) Rectal cancer, version 2.2018, NCCN clinical practice guidelines in oncology. J Natl Compr Canc Netw 16:874–901

2. Chang GJ, Rodriguez-Bigas MA, Skibber JM, Moyer VA (2007) Lymph node evaluation and survival after curative resection of colon cancer: systematic review. J Natl Cancer Inst 99:433–441

3. Kim JH, Beets GL, Kim MJ, Kessels AG, Beets-Tan RG (2004) High-resolution MR imaging for nodal staging in rectal cancer: are there any criteria in addition to the size? Eur J Radiol 52:78–83

4. Zhang H, Zhang C, Zheng Z et al (2017) Chemical shift effect predicting lymph node status in rectal cancer using high-resolution MR imaging with node-for-node matched histopathological validation. Eur Radiol 27:3845–3855

5. Brown G, Richards CJ, Bourne MW et al (2003) Morphologic predictors of lymph node status in rectal cancer with use of high-spatial-resolution MR imaging with histopathologic comparison. Radiology 227:371–377

6. Glynne-Jones R, Wyrwicz L, Tiret E et al (2017) Rectal cancer: ESMO clinical practice guidelines for diagnosis, treatment and follow-up. Ann Oncol 28:iv22–iv40

7. Schurink NW, Lambregts DMJ, Beets-Tan RGH (2019) Diffusion-weighted imaging in rectal cancer: current applications and future perspectives. Br J Radiol 92:20180655

8. Cerny M, Dunet V, Prior JO et al (2016) Initial staging of locally advanced rectal cancer and regional lymph nodes: comparison of diffusion-weighted MRI with 18F-FDG-PET/CT. Clin Nucl Med 41:289–295

9. Kim SH, Yoon JH, Lee Y (2015) Added value of morphologic characteristics on diffusion-weighted images for characterizing lymph nodes in primary rectal cancer. Clin Imaging 39:1046–1051

10. Lambregts DM, Maas M, Riedl RG et al (2011) Value of ADC measurements for nodal staging after chemoradiation in locally advanced rectal cancer-a per lesion validation study. Eur Radiol 21:265–273

11. Heijnen LA, Lambregts DM, Mondal D et al (2013) Diffusion-weighted MR imaging in primary rectal cancer staging demonstrates but does not characterise lymph nodes. Eur Radiol 23:3354–3360

12. Lee AS, Weissleder R, Brady TJ, Wittenberg J (1991) Lymph nodes: microstructural anatomy at MR imaging. Radiology 178:519–522

13. Schnall MD, Furth EE, Rosato EF, Kressel HY (1994) Rectal tumor stage: correlation of endorectal MR imaging and pathologic findings. Radiology 190:709–714

14. Tang Y, Rao S, Yang C, Hu Y, Sheng R, Zeng M (2018) Value of MRI morphologic features with pT1-2 rectal cancer in determining lymph node metastasis. J Surg Oncol 118:544–550

15. Nöth U, Shrestha M, Schüre JR, Deichmann R (2017) Quantitative in vivo T2 mapping using fast spin echo techniques - a linear correction procedure. Neuroimage 157:476–485

16. Wang F, Zhang H, Wu C et al (2019) Quantitative T2 mapping accelerated by GRAPPATINI for evaluation of muscles in patients with myositis. Br J Radiol 92:20190109

17. Huang L, Ran L, Zhao P et al (2019) MRI native T1 and T2 mapping of myocardial segments in hypertrophic cardiomyopathy: tissue remodeling manifested prior to structure changes. Br J Radiol 92:20190634

18. Sollmann N, Weidlich D, Cervantes B et al (2019) High isotropic resolution T2 mapping of the lumbosacral plexus with T2-prepared 3D turbo spin echo. Clin Neuroradiol 29:223–230

19. Wu Q, Zhu LN, Jiang JS, Bu SS, Xu XQ, Wu FY (2020) Characterization of parotid gland tumors using T2 mapping imaging: initial findings. Acta Radiol 61:629–635

20. Liu L, Yin B, Shek K et al (2018) Role of quantitative analysis of T2 relaxation time in differentiating benign from malignant breast lesions. J Int Med Res 46:1928–1935

21. Mai J, Abubrig M, Lehmann T et al (2019) T2 mapping in prostate cancer. Invest Radiol 54:146–152

22. Yu XP, Wen L, Hou J, Wang H, Lu Q (2016) Discrimination of metastatic from non-metastatic mesorectal lymph nodes in rectal cancer using quantitative dynamic contrast-enhanced magnetic resonance imaging. J Huazhong Univ Sci Technolog Med Sci 36:594–600

23. Cho EY, Kim SH, Yoon JH et al (2013) Apparent diffusion coefficient for discriminating metastatic from non-metastatic lymph nodes in primary rectal cancer. Eur J Radiol 82:e662–e668

24. Yang X, Chen Y, Wen Z et al (2019) Non-invasive MR assessment of the microstructure and microcirculation in regional lymph nodes for rectal cancer: a study of intravoxel incoherent motion imaging. Cancer Imaging 19:70

25. Chaland B, Mariette F, Marchal P, De Certaines J (2000) 1H nuclear magnetic resonance relaxometric characterization of fat and water states in soft and hard cheese. J Dairy Res 67:609–618

26. Zaman A, Higgins DM, Motwani M et al (2015) Robust myocardial T2 and T2 * mapping at 3T using image-based shimming. J Magn Reson Imaging 41:1013–1020

27. Ishibe A, Ota M, Watanabe J et al (2016) Prediction of lateral pelvic lymph-node metastasis in low rectal cancer by magnetic resonance imaging. World J Surg 40:995–1001

28. Roccia E, Vidya Shankar R, Neji R et al (2019) Accelerated 3D T2 mapping with dictionary-based matching for prostate imaging. Magn Reson Med 81:1795–1805

29. Yamada I, Yoshino N, Hikishima K et al (2017) Colorectal carcinoma: ex vivo evaluation using 3-T high-spatial-resolution quantitative T2 mapping and its correlation with histopathologic findings. Magn Reson Imaging 38:174–181